Improving the Convergence of the Doublet-Lattice Method Through Tip Corrections

Myles L. Baker
Senior Engineer, Loads and Dynamics
The Boeing Company
Long Beach, California 90807-5608, USA
myles.l.baker@boeing.com

William P. Rodden
Consulting Engineer
William P. Rodden, Ph.D., Inc.
La Canada Flintridge, California 92011-2831, USA
billrodden@aol.com

In 1973 Hough studied the slow convergence of the Vortex-Lattice Method (VLM) as the number of spanwise divisions (strips) is increased. Specifically, the lift curve slope of a lifting surface was shown to decrease significantly as the resolution of the lattice was increased, converging to the "true" value only with relatively fine spanwise divisions. Impressive improvements in the converged results were achieved when equally spaced divisions of the lifting surface were inset from the tip by a fraction of the strip width. Hough demonstrated the improvement via the tip inset on a number of wing planforms at a constant angle of attack.

Hough's argument was based on an elliptical lift distribution which is a reasonable assumption in the steady, symmetric case. The present paper investigates also cases where elliptical lift distributions are not expected, specifically, the antisymmetric motion of rolling, elastic motions, and oscillatory motions with high reduced frequencies. The beneficial effect of the tip inset is observed in all cases investigated

Keywords: Doublet, Lattice, Unsteady Aerodynamics, Convergence

1. Introduction

Following a suggestion of Rubbert[1] that equally spaced divisions on a lifting surface should be inset from the tip by a fraction d ($0<d<1$) of the strip width,, Hough [2,3] has demonstrated impressive improvement in the estimation of lift curve slope ($C_{L\alpha}$) of a wing without using an inordinate number of spanwise strips, specifically for d = ¼. The tip inset concept is illustrated in Figure 1, and some of Hough's convergence results for $C_{L\alpha}$ are shown in Figure 2.

Hough's recommendation of d = ¼ was based on an analysis of an elliptical lift distribution which is typical of a steady symmetrical aerodynamic loading. It is the purpose of this paper to investigate

the convergence improvement that can be obtained by applying the tip inset correction to the oscillatory Doublet-Lattice Method (DLM, which reduces to the VLM in the steady case) for conditions in which elliptical lift distributions are not expected

The tip correction is implemented by reducing the effective span of the wing (the span that is actually paneled with Doublet-Lattice boxes) by the factor NS/(NS+d), where NS is the number of spanwise strips, and d is the tip inset factor (typically ¼). The lack of an aerodynamic panel on the most outboard tip of the wing has the effect of driving the tip loading toward the correct value of zero. Since the DLM assumes constant loading (spanwise) within a box, it requires a very high resolution to capture the correct wingtip load distribution, and the DLM will typically over-predict the tip loading, and approach the correct results from above as the resolution is refined.

2. Results

Rectangular Wings: Two wings pitching about their midchords at a Mach number of M=0.80 are studied. The first wing has aspect ratio of AR=2. It is divided into various numbers of spanwise strips (NS), and various numbers of chordwise boxes (NC) such that the maximum box aspect ratio is less than 8.0. The value of NC necessary for convergence depends on the reduced frequency $k_r=\omega c/2V$, where ω is the angular frequency (rad/sec), c is the reference chord (c = 1.0 for the rectangular wings), and V is the freestream velocity. The guideline of Ref. 5 recommends 50 boxes per wavelength λ, where $\lambda = \pi c/k_r$.

The steady lift curve slope $C_{L\alpha}$ and the roll damping coefficient C_{lp} are obtained from the DLM at $k_r=0.001$. Oscillatory results are obtained for $k_r=0.1$, 0.5, 1.0, and 2.0. The results for the aspect ratio 2 wing are presented in Figures 3 and 4. Figure 3 shows the results for the symmetric case (lift curve slope), and Figure 4 shows the antisymmetric (roll damping coefficient) results. Figures 3 and 4 present the real parts on the left and the imaginary parts on the right. The solid lines are the results with the tip correction applied, and the dashed lines are the results without the tip correction. The data are plotted as functions of the reciprocal of the number of spanwise strips, so that extrapolation of 1/NS to zero should provide converged results. The steady case (based on $k_r=0.001$) is shown at the tops of the figures, with results for increasing reduced frequencies shown below. As the reduced frequency is increased, more chordwise boxes are required to satisfy the requirement of 50 boxes per wavelength. The figures only present data that satisfy the requirement.

Perusing Figure 3 from top to bottom, we make the following observations in the symmetric case. The top graph is the steady case and the convergence with the tip correction behaves as Hough has shown[2,3]. The next two graphs below are for $k_r=0.1$ and good convergence with the tip correction is found for the real part and significant improvement is seen in the imaginary part. The next two graphs are for $k_r=0.5$ and some dependence on the number of chordwise boxes appears, but both real and imaginary parts are improved with the tip correction over the results without it. Similar behavior is seen in the remaining graphs for $k_r=1.0$ and 2.0: There is some dependence on the number of chordwise boxes, and the tip correction improves the results but moreso in the real part than the imaginary part.

Figure 4 is similar to Figure 3 but for the antisymmetric case. The top graph is the steady damping-in-roll coefficient. Again, as in the symmetric case, the tip correction leads to converged results almost independent of the number of spanwise strips. Below the steady case is the damping-in-roll coefficient at $k_r=0.1$. Both real and imaginary parts are improved with the tip correction. Both real

and imaginary parts are improved with the tip correction also at k_r=0.5. At the higher reduced frequencies of k_r=1.0 and 2.0, the damping-in-roll coefficient exhibits some dependence on the number of chordwise boxes, but this dependence is less than that seen above in the symmetric case and the tip correction leads to better results.

The second wing has an aspect ratio of 7.0. As in the AR=2.0 case, the wing was analyzed in both symmetric and antisymmetric oscillatory rigid body motion. The results are presented in Tables 1 and 2. Table 1 contains the symmetric results, and Table 2 presents the results of the antisymmetric analysis. A tabular presentation of these results is made to give the reader a different perspective on the data from the graphical format (Note that tabulated results of the data for the figures in this paper are available from the authors). Blank entries in the tables indicate that the combination of NC and k_r do not satisfy the wavelength requirement.

The results in Tables 1 and 2 for the aspect ratio 7.0 rectangular wing are similar to the results plotted in Figures 3 and 4 for the aspect ratio 2.0 rectangular wing. The steady lift curve slope in Table 1 (found at k_r=0.001) is again found to be reasonably constant with the number of spanwise strips when the tip correction is made. At k_r=0.1, the oscillatory lift curve slope computed with the tip correction is also fairly constant with the number of strips. At k_r=0.5, the real parts with the tip correction are again insensitive to the number of spanwise strips, but there is some dependence of the imaginary parts on the number of chordwise boxes. Also, the variation in the imaginary parts is about the same whether or not the tip correction is made. At k_r=1.0 and 2.0, the real parts are again improved with the tip correction, but the imaginary parts are not significantly affected by it. As in the aspect ratio 2.0 results, a dependence on the number of chordwise boxes is observed.

In Table 2, the antisymmetric results follow the pattern of the symmetric case. The steady damping-in-roll coefficient is much improved by the tip correction. At all of the higher reduced frequencies, it is the real parts that are improved by the tip correction. At the low reduced frequency k_r=0.1, the tip correction improved the imaginary parts, especially for a small number of chordwise boxes (NC=10 and 20), but at the high frequencies, the tip correction does not have much effect on the imaginary parts.

LANN Wing: In order to investigate the convergence behavior of aeroelastic generalized forces as the box resolution is refined, a model with realistic elastic vibration modes is required. These generalized forces are extremely important in flutter and aeroservoelastic analysis. The LANN wing[6], which was chosen for this study, is a well-published sample case representative of a high aspect ratio transport wing, and is complete with elastic modal data. The wing has an aspect ratio of 7.9, a taper ratio of 0.40, and a leading edge sweep of 27.5 degrees. The first bending and first torsion mode shapes of the LANN wing are shown in Figure 5.

The unsteady generalized aerodynamic forces for the two mode shapes shown in Figure 5 were computed at reduced frequencies of k_r=0.01, 0.5,.1.0, and 2.0 for varying numbers of spanwise strips and chordwise boxes. The number of spanwise strips varied from 5 to 20, and the number of chordwise boxes varied from 5 to 25. Figure 6 shows the Generalized Aerodynamic Force coefficient (GAF) in first wing bending in a similar format to that used for the rectangular wing results discussed above. The top pair of graphs in Figure 6 show the real and imaginary parts of the GAF in first wing bending at a reduced frequency of k_r=0.01. As seen in the rigid symmetric and antisymmetric results for the rectangular wings, the generalized aerodynamic forces at this low reduced frequency are rendered almost independent of the number of spanwise strips through the

use of the tip correction. This observation applies to both the real and imaginary parts. The next set of graphs in Figure 6 show the results for a reduced frequency of k_r=0.5. Again, the convergence of the results is improved dramatically through the use of the tip correction. Note that there is some dependence of the real part of the GAF on the number of chordwise boxes. The next two pairs of graphs show the results for reduced frequencies of k_r=1.0 and 2.0. In each case, the real part of the GAF is either slightly improved or unaffected by the application of the tip correction, while the imaginary part is not significantly improved. In fact, at k_r=2.0, it appears that the tip correction offers a slight reduction in convergence properties. However, this is more than offset by the dramatic improvements seen in the other conditions.

Figure 7 shows the results for the first torsion mode of the LANN wing. In this case, the effect of the tip inset correction is much smaller. The real parts of the GAF's at all reduced frequencies are slightly improved, while the convergence of the imaginary parts is slightly reduced. The overall result is that the tip correction is not an obvious improvement in this case, but it is clearly not detrimental to convergence.

3. Concluding Remarks

The foregoing discussions of the results for the three configurations may be summarized as follows. In general, the tip inset correction improves the convergence by decreasing the sensitivity of the results to the number of spanwise strips. This is observed for both symmetric and antisymmetric rigid body motions of rectangular wings in both the steady and oscillatory cases up to a reduced frequency of 2.0. It is also observed in the case of oscillatory symmetric elastic modes of a swept, tapered wing representative of a subsonic transport.

The observations above are general, but some specific features may be pointed out. The improvement in the steady lift curve slope is observed again as Hough has shown before [2,3]. A comparable improvement in the steady roll damping coefficient is found here. However, as the frequency increases, the effectiveness of the correction is somewhat reduced. The tip inset correction also appears to be more effective in improving the real part of the unsteady aerodynamic forces than the imaginary part (although the benefits to the imaginary part are substantial in most cases).

There is sufficient benefit to the tip inset correction in all cases studied to make the recommendation that it be used routinely, particularly since the correction is so easily made. Only the case of equal width spanwise strips has been considered. Other spanwise distributions of strip width require further investigation.

4. References

1. P. E. Rubbert, "Theoretical Characteristics of Arbitrary Wings by a Non-Planar Vortex Lattice Method," D6-9244, 1964, The Boeing Co., Renton, WA.

2. G. R. Hough, "Remarks on Vortex-Lattice Methods," J. Aircraft, Vol. 10, No. 5, 1973, pp. 314-317.

3. G. R. Hough, "Lattice Arrangement for Rapid Convergence," Vortex-Lattice Utilization, NASA SP-405, Mat 17-18, 1976, pp. 325-342.

4. W. P. Rodden, P. F. Taylor, S. C. McIntosh, Jr., "Further Refinement of the Nonplanar Aspects of the Subsonic Doublet-Lattice Lifting Surface Method," 20th Congress of the International Council of the Aeronautical Sciences, Paper ICAS 96-2.8.2, September 1996, also *J. Aircraft*, Vol. 35, No. 5, 1998, pp. 720-727.

5. W. P. Rodden, P. F. Taylor, S. C. McIntosh, and M. L. Baker, "Further Convergence Studies of the Enhanced Subsonic Doublet-Lattice Oscillatory Lifting Surface Method," International Forum of Aeroelasticity and Structural Dynamics, 17-20 June 1997, Rome, Italy, pp. 401-408, to be published in *J. Aircraft*.

6. Horsten, J.J., den Boer, R. G., and Zwaan, R. J., "Unsteady Transonic Pressure Measurements on a Semispan Wind Tunnel Model of a Transport-Type Supercritical Wing (LANN Model), Part I," Air Force Wright Aeronautical Laboratory, Report AFWAL-TR-83-3039, March 1983.

No Tip Correction					
NS	**k_r=0.001**	**k_r=0.1**	**k_r=0.5**	**k_r=1.0**	**k_r=2.0**
5	**6.553**	**5.892-0.769i**	**4.882+0.325i**		
10	**6.358**	**5.735-0.733i**	**4.814+0.268i**		
20	**6.255**	**5.651-0.711i**	**4.753+0.270i**		
Tip Correction					
NS	**k_r=0.001**	**k_r=0.1**	**k_r=0.5**	**k_r=1.0**	**k_r=2.0**
5	**6.117**	**5.545-0.670i**	**4.637+0.322i**		
10	**6.139**	**5.561-0.683i**	**4.688+0.271i**		
20	**6.145**	**5.564-0.686i**	**4.689+0.272i**		

Table 1(a): Symmetric (lift curve slope) convergence behavior for aspect ratio 7.0 rectangular wing with 10 Chordwise Boxes

No Tip Correction					
NS	**k_r=0.001**	**k_r=0.1**	**k_r=0.5**	**k_r=1.0**	**k_r=2.0**
9	**6.381**	**5.755-0.741i**	**4.845+0.240i**	**5.021+0.814i**	
15	**6.290**	**5.681-0.727i**	**4.815+0.205i**	**4.979+0.725i**	
20	**6.255**	**5.653-0.720i**	**4.800+0.196i**	**4.958+0.702i**	
Tip Correction					
NS	**k_r=0.001**	**k_r=0.1**	**k_r=0.5**	**k_r=1.0**	**k_r=2.0**
9	**6.138**	**5.561-0.686i**	**4.706+0.243i**	**4.885+0.795i**	
15	**6.144**	**5.565-0.693i**	**4.730+0.208i**	**4.897+0.718i**	
20	**6.145**	**5.566-0.695i**	**4.736+0.198i**	**4.896+0.698i**	

Table 1(b): Symmetric (lift curve slope) convergence behavior for aspect ratio 7.0 rectangular wing with 20 Chordwise Boxes

No Tip Correction					
NS	k_r=0.001	k_r=0.1	k_r=0.5	k_r=1.0	k_r=2.0
14	6.300	5.690-0.729i	4.824+0.199i	4.991+0.714i	
20	6.255	5.654-0.722i	4.809+0.181i	4.968+0.669i	
25	6.234	5.637-0.719i	4.801+0.174i	4.956+0.652i	
Tip Correction					
NS	k_r=0.001	k_r=0.1	k_r=0.5	k_r=1.0	k_r=2.0
14	6.143	5.565-0.693i	4.733+0.202i	4.903+0.705i	
20	6.145	5.567-0.697i	4.745+0.183i	4.906+0.665i	
25	6.146	5.567-0.699i	4.750+0.176i	4.907+0.649i	

Table 1(c): Symmetric (lift curve slope) convergence behavior for aspect ratio 7.0 rectangular wing with 30 Chordwise Boxes

No Tip Correction					
NS	k_r=0.001	k_r=0.1	k_r=0.5	k_r=1.0	k_r=2.0
18	6.267	5.663-0.725i	4.815+0.181i	4.977+0.672i	5.913+0.728i
25	6.234	5.637-0.720i	4.805+0.167i	4.960+0.638i	5.907+0.660i
30	6.220	5.626-0.717i	4.799+0.162i	4.952+0.626i	5.902+0.636i
Tip Correction					
NS	k_r=0.001	k_r=0.1	k_r=0.5	k_r=1.0	k_r=2.0
18	6.145	5.566-0.697i	4.745+0.184i	4.909+0.666i	5.831+0.717i
25	6.146	5.567-0.699i	4.753+0.170i	4.910+0.635i	5.848+0.654i
30	6.147	5.568-0.701i	4.756+0.164i	4.911+0.624i	5.853+0.632i

Table 1(d): Symmetric (lift curve slope) convergence behavior for aspect ratio 7.0 rectangular wing with 40 Chordwise Boxes

No Tip Correction					
NS	k_r=0.001	k_r=0.1	k_r=0.5	k_r=1.0	k_r=2.0
22	6.245	5.646-0.722i	4.810+0.170i	4.967+0.645i	5.914+0.671i
30	6.220	5.626-0.718i	4.801+0.159i	4.954+0.619i	5.908+0.617i
35	6.209	5.618-0.716i	4.797+0.155i	4.948+0.610i	5.905+0.599i
Tip Correction					
NS	k_r=0.001	k_r=0.1	k_r=0.5	k_r=1.0	k_r=2.0
22	6.146	5.567-0.699i	4.752+0.173i	4.911+0.641i	5.847+0.663i
30	6.147	5.568-0.701i	4.758+0.161i	4.913+0.616i	5.859+0.613i
35	6.147	5.568-0.702i	4.760+0.157i	4.913+0.608i	5.863+0.595i

Table 1(e): Symmetric (lift curve slope) convergence behavior for aspect ratio 7.0 rectangular wing with 50 Chordwise Boxes

No Tip Correction					
NS	**k_r=0.001**	**k_r=0.1**	**k_r=0.5**	**k_r=1.0**	**k_r=2.0**
5	**-0.6763**	**-0.6753-0.0112i**	**-0.6639-0.0549i**		
10	**-0.6312**	**-0.6308-0.0135i**	**-0.6314-0.0555i**		
20	**-0.6062**	**-0.6061-0.0143i**	**-0.6097-0.0573i**		
Tip Correction					
NS	**kr=0.001**	**kr=0.1**	**kr=0.5**	**kr=1.0**	**kr=2.0**
5	**-0.5646**	**-0.5753-0.0146i**	**-0.5703-0.0549i**		
10	**-0.5760**	**-0.5760-0.0148i**	**-0.5845-0.0557i**		
20	**-0.5789**	**-0.5789-0.0150i**	**-0.5864-0.0573i**		

Table 2(a): Antisymmetric (roll damping) convergence behavior for aspect ratio 7.0 rectangular wing with 10 Chordwise Boxes

No Tip Correction					
NS	**k_r=0.001**	**k_r=0.1**	**k_r=0.5**	**k_r=1.0**	**k_r=2.0**
9	**-0.6366**	**-0.6363-0.0131i**	**-0.6385-0.0525i**		
15	**-0.6148**	**-0.6148-0.0138i**	**-0.6226-0.0510i**		
20	**-0.6064**	**-0.6064-0.0140i**	**-0.6160-0.0507i**		
Tip Correction					
NS	**k_r=0.001**	**k_r=0.1**	**k_r=0.5**	**k_r=1.0**	**k_r=2.0**
5	**-0.5751**	**-0.5753-0.0146i**	**-0.5862-0.0528i**		
10	**-0.5782**	**-0.5785-0.0146i**	**-0.5913-0.0513i**		
20	**-0.5790**	**-0.5793-0.0146i**	**-0.5925-0.0510i**		

Table 2(b): Antisymmetric (roll damping) convergence behavior for aspect ratio 7.0 rectangular wing with 20 Chordwise Boxes

No Tip Correction					
NS	**k_r=0.001**	**k_r=0.1**	**k_r=0.5**	**k_r=1.0**	**k_r=2.0**
14	**-0.6172**	**-0.6172-0.0137i**	**-0.6251-0.0504i**	**-0.6243-0.1265i**	
20	**-0.6064**	**-0.6065-0.0139i**	**-0.6172-0.0493i**	**-0.6153-0.1223i**	
25	**-0.6012**	**-0.6015-0.0140i**	**-0.6132-0.0489i**	**-0.6109-0.1206i**	
Tip Correction					
NS	**k_r=0.001**	**k_r=0.1**	**k_r=0.5**	**k_r=1.0**	**k_r=2.0**
14	**-0.5780**	**-0.5783-0.0146i**	**-0.5916-0.0507i**	**-0.5906-0.1208i**	
20	**-0.5790**	**-0.5794-0.0145i**	**-0.5937-0.0496i**	**-0.5918-0.1185i**	
25	**-0.5794**	**-0.5798-0.0145i**	**-0.5945-0.0492i**	**-0.5921-0.1176i**	

Table 2(c): Antisymmetric (roll damping) convergence behavior for aspect ratio 7.0 rectangular wing with 30 Chordwise Boxes

No Tip Correction					
NS	**k_r=0.001**	**k_r=0.1**	**k_r=0.5**	**k_r=1.0**	**k_r=2.0**
18	**-0.6092**	**-0.6093-0.0138i**	**-0.6196-0.0492i**	**-0.6181-0.1227i**	**-0.7314-0.2080i**
25	**-0.6012**	**-0.6015-0.0140i**	**-0.6137-0.0484i**	**-0.6115-0.1194i**	**-0.7250-0.2011i**
30	**-0.5977**	**-0.5980-0.0140i**	**-0.6110-0.0481i**	**-0.6086-0.1181i**	**-0.7219-0.1986i**
Tip Correction					
NS	**k_r=0.001**	**k_r=0.1**	**k_r=0.5**	**k_r=1.0**	**k_r=2.0**
18	**-0.5788**	**-0.5791-0.0145i**	**-0.5935-0.0496i**	**-0.5920-0.1184i**	**-0.7011-0.2002i**
25	**-0.5794**	**-0.5798-0.0145i**	**-0.5950-0.0487i**	**-0.5927-0.1164i**	**-0.7032-0.1958i**
30	**-0.5796**	**-0.5800-0.0145i**	**-0.5954-0.0483i**	**-0.5929-0.1156i**	**-0.7037-0.1942i**

Table 2(d): Antisymmetric (roll damping) convergence behavior for aspect ratio 7.0 rectangular wing with 40 Chordwise Boxes

No Tip Correction					
NS	**k_r=0.001**	**k_r=0.1**	**k_r=0.5**	**k_r=1.0**	**k_r=2.0**
22	**-0.6040**	**-0.6043-0.0139i**	**-0.6160-0.0484i**	**-0.6141-0.1201i**	**-0.7281-0.2024i**
30	**-0.5977**	**-0.5981-0.0140i**	**-0.6113-0.0478i**	**-0.6089-0.1174i**	**-0.7231-0.1968i**
35	**-0.5952**	**-0.5956-0.0141i**	**-0.6094-0.0475i**	**-0.6068-0.1165i**	**-0.7209-0.1948i**
Tip Correction					
NS	**k_r=0.001**	**k_r=0.1**	**k_r=0.5**	**k_r=1.0**	**k_r=2.0**
22	**-0.5792**	**-0.5796-0.0145i**	**-0.5947-0.0488i**	**-0.5927-0.1166i**	**-0.7033-0.1962i**
30	**-0.5796**	**-0.5800-0.0144i**	**-0.5957-0.0480i**	**-0.5932-0.1150i**	**-0.7049-0.1924i**
35	**-0.5797**	**-0.5802-0.0144i**	**-0.5960-0.0477i**	**-0.5934-0.1144i**	**-0.7053-0.1911i**

Table 2(e): Antisymmetric (roll damping) convergence behavior for aspect ratio 7.0 rectangular wing with 50 Chordwise Boxes

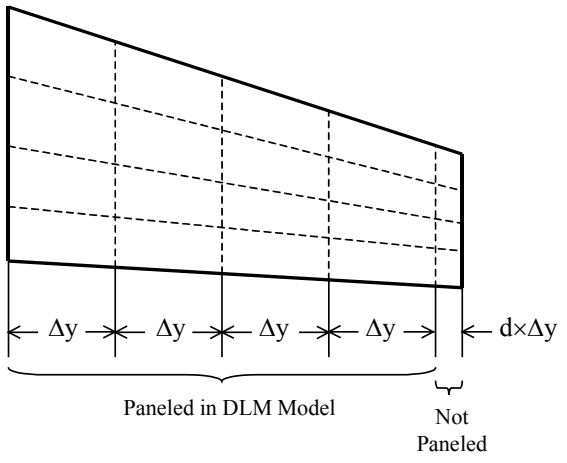

Figure 1: Tip Inset Illustration.

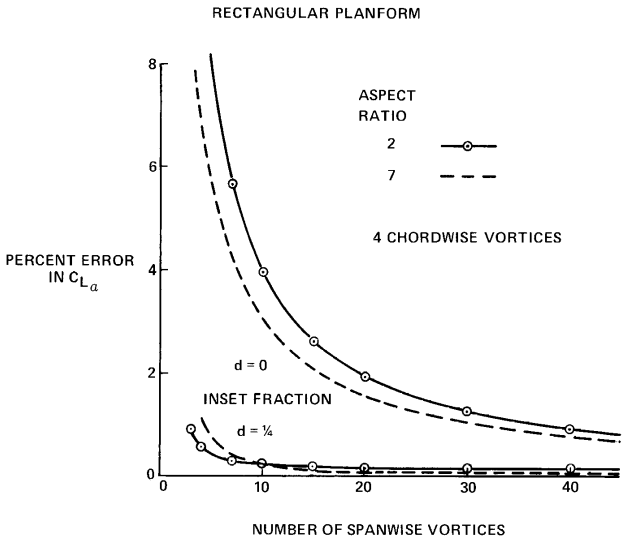

Figure 2: Effect of Tip Inset on Steady $C_{L\alpha}$ (Hough[2]).

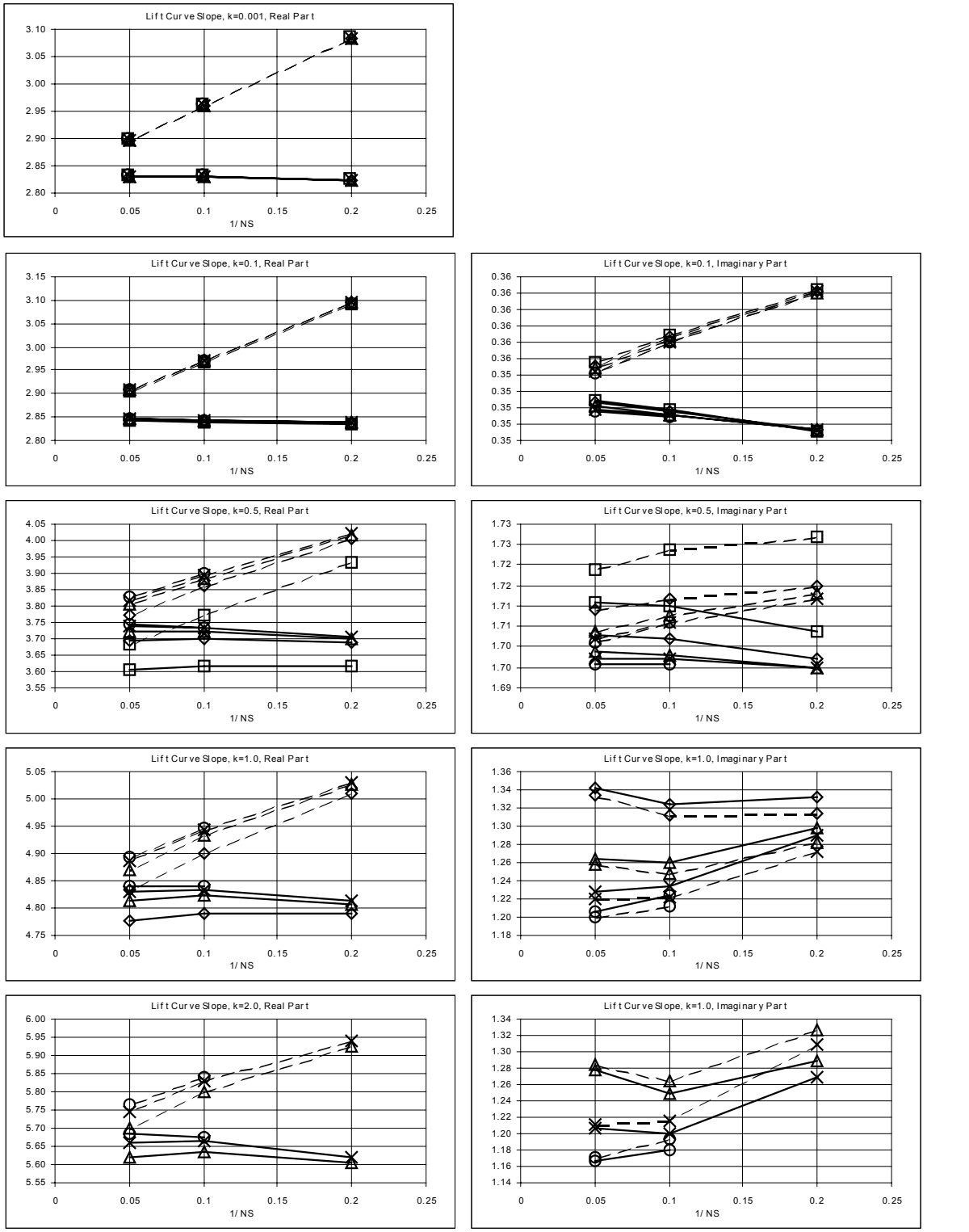

Figure 3: Convergence behavior of Lift due to pitching oscillations for the AR 2 rectangular wing. Real part on left, Imaginary part on Right.

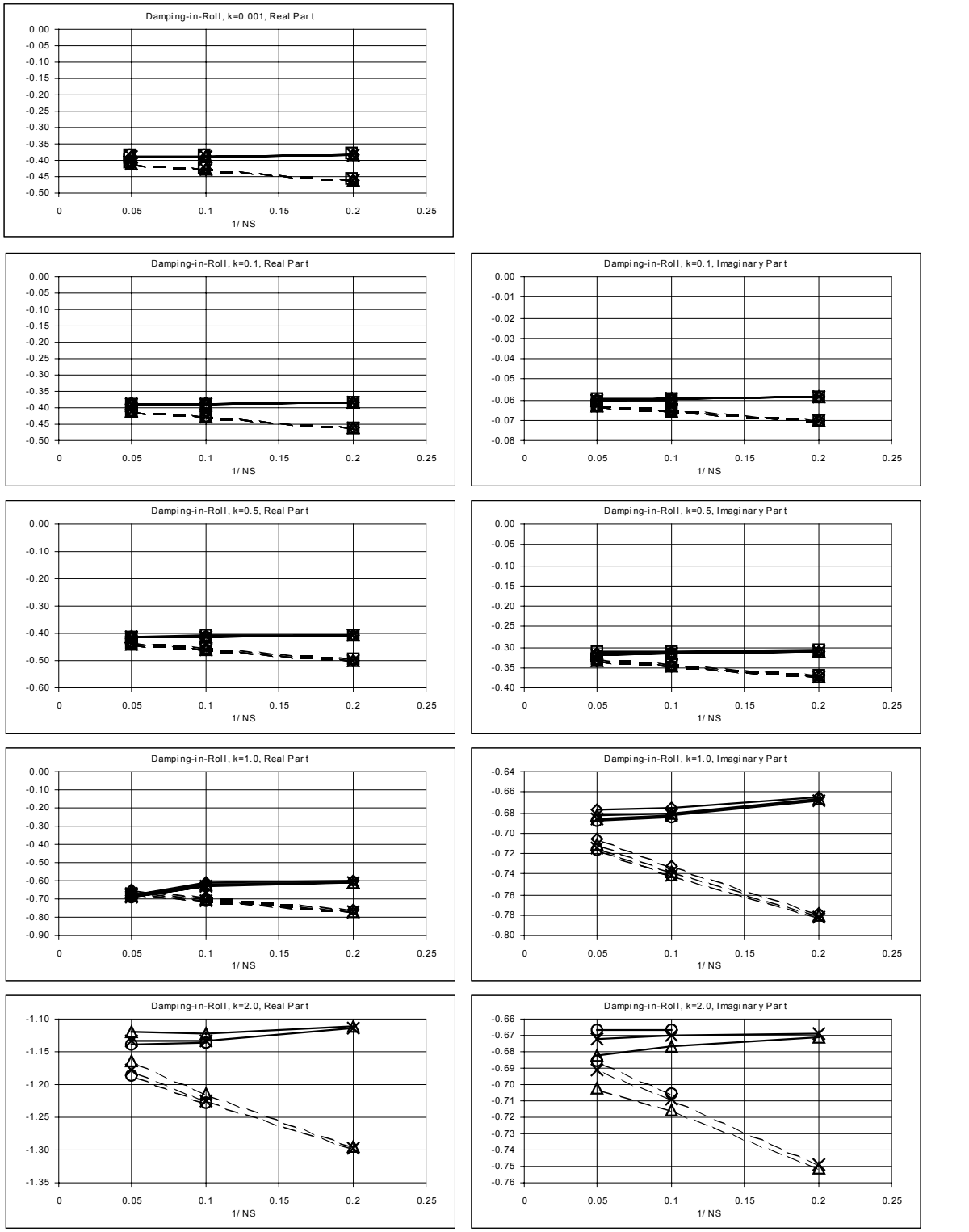

Figure 4: Convergence behavior of Rolling moment due to roll oscillations for the AR 2 rectangular wing. Real part on left, Imaginary part on Right.

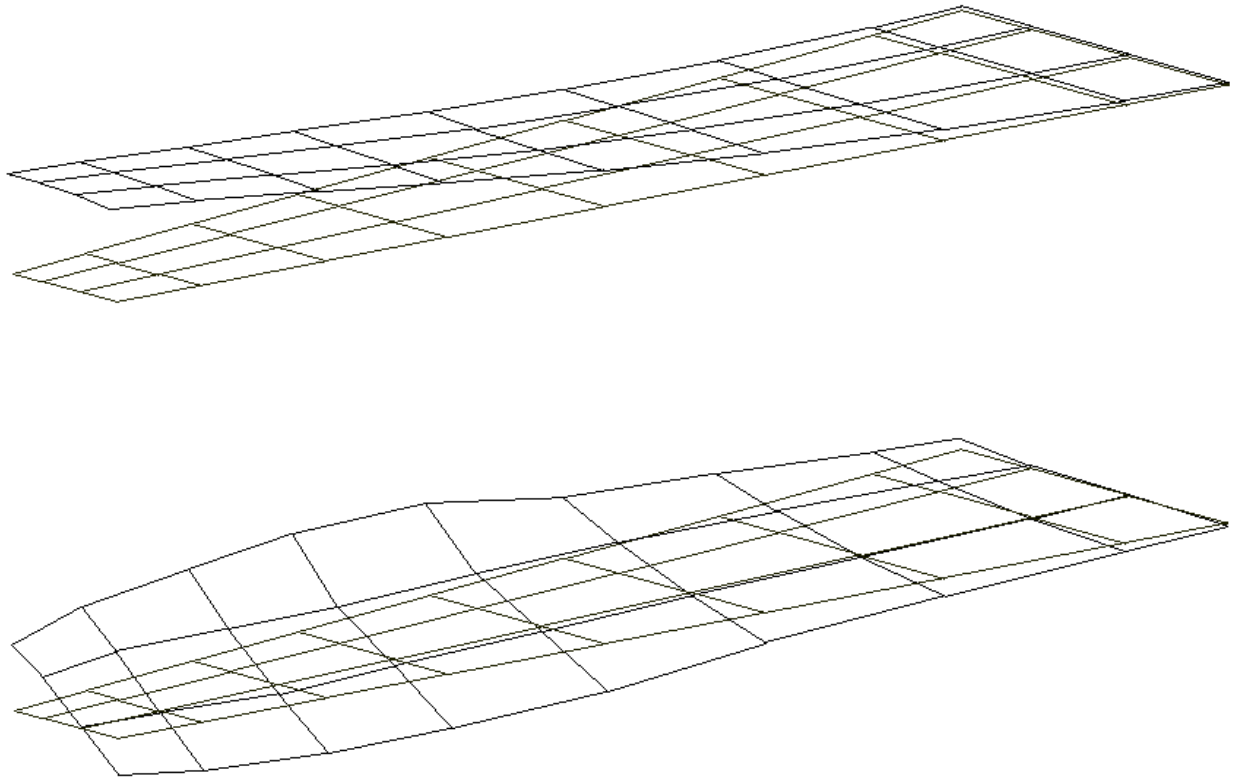

Figure 5: LANN Wing: First Bending and Torsion Mode Shapes.

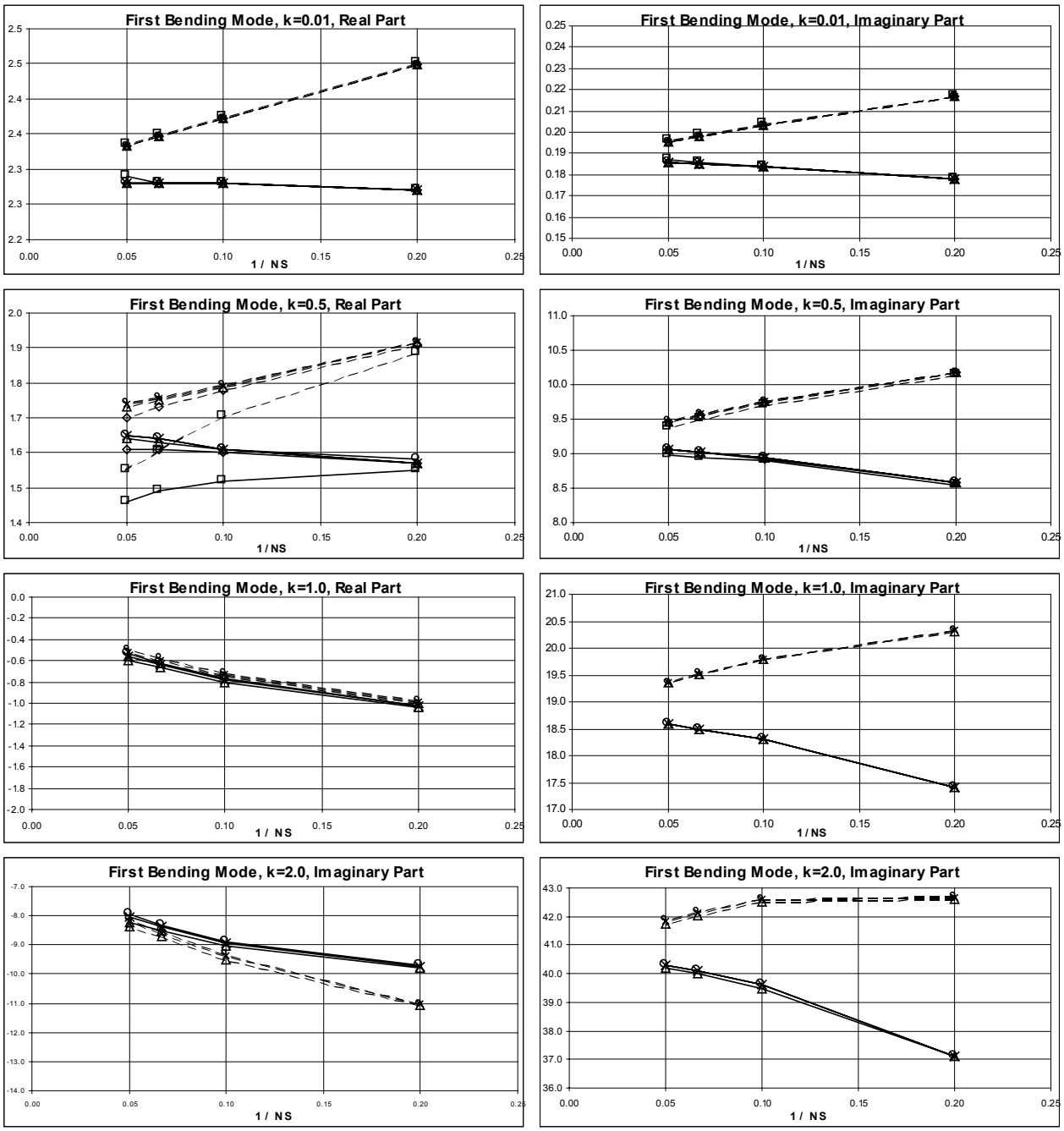

Figure 6: Convergence behavior of generalized aerodynamic force in first bending mode due to first bending mode excitation. Variation in chordwise boxes, spanwise strips, and tip configuration is shown vs. reduced frequency.

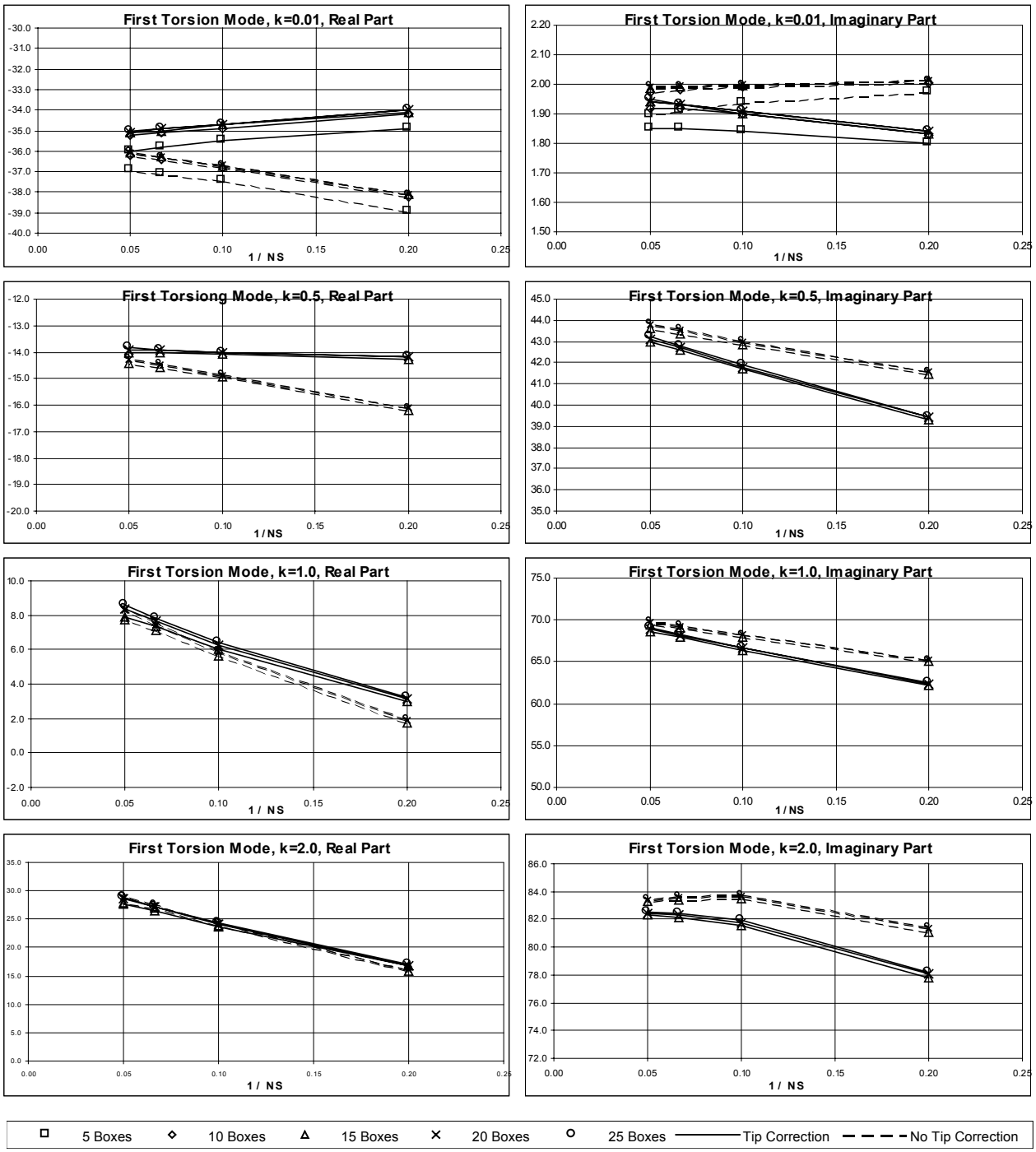

Figure 7: Convergence behavior of generalized aerodynamic force in first torsion mode due to first torsion mode excitation. Variation in chordwise boxes, spanwise strips, and tip configuration is shown vs. reduced frequency.